

Spin excitations of magnetic vortices in ferromagnetic nanodotsV. Novosad,¹ M. Grimsditch,¹ K. Yu. Guslienko,² P. Vavassori,³ Y. Otani,^{4,5} and S. D. Bader¹¹*Materials Science Division, Argonne National Laboratory, Argonne, Illinois 60439*²*Seagate Research, Pittsburgh, Pennsylvania 15222*³*INFN-Dipartimento di Fisica, Universita di Ferrara, I-44100, Italy*⁴*RIKEN, Frontier Research System, Wako 351-0198, Japan*⁵*Japan Science & Technology Corporation, CREST, Japan*

(Received 23 February 2002; published 9 August 2002)

Spin excitations of the magnetic vortex state in ferromagnetic nanodots are measured using Brillouin light scattering. Arrays of permalloy dots with 800-nm diameter and 60-nm thickness were fabricated by means of electron beam lithography and lift-off procedures. Two excitation modes are observed experimentally in the vortex state. One mode, at ~ 12 GHz, decreases slightly in frequency to 11 GHz as an in-plane magnetic field is applied. The lower mode, at ~ 8 GHz, is almost independent of applied field strength. Numerical and analytical calculations of the dynamic magnetization based on the Landau-Lifshitz equation of motion allows us to identify the higher and lower frequency modes as corresponding to dipole-dominated spin excitations localized inside the dot and at the dot edges, respectively.

DOI: 10.1103/PhysRevB.66.052407

PACS number(s): 75.75.+a, 76.50.+g, 78.35.+c

Although predicted many decades ago the magnetic vortex state has recently received renewed attention since it is often found to be the ground state of nanopatterned magnetic particles. There is already a substantial number of investigations where the stability of the vortex state has been investigated with regard to the sample shape and size and also the presence of an external field.^{1–10} To complement our fundamental understanding of the vortex state, here we present an investigation of spin-wave excitations within the vortex state. This investigation is thus part of the much wider effort which is currently being directed at understanding high-frequency magnetization dynamics in small magnetic elements. Such investigations are not only a challenge for modern magnetism theory, but are also important for developing high-density magnetic recording media, where nanosecond duration field pulses are applied to induce magnetization reversal.

The ground-state spin distribution at zero field within a ferromagnet with negligibly small magnetocrystalline anisotropy depends on both the size and shape of the material.¹ The exchange energy is smallest for parallel alignment of neighboring spins and therefore favors a uniform magnetization distribution, the single domain state. However, collinear spin alignments usually lead to large demagnetizing fields that increase the magnetostatic energy and hence favors flux closure or multiple domain states to reduce them. The size at which a particle becomes a single domain depends on the balance between the above energies, and also on its shape and magnetic anisotropy. The characteristic magnetic exchange length resulting from the above energy competition is defined as $\xi_{\text{ex}} = \sqrt{2A/M_s}$, where A is the exchange stiffness constant and M_s is the saturation magnetization. The competition between different energies leads to the nonuniform magnetic state (“magnetization curling”) that appears as a type of spin instability during the magnetization reversal process. Under some conditions, this is the lowest eigenmode of Brown’s equations for systems with cylindrical symmetry.^{2,3} The “curling magnetization distribution,” also referred to as

a magnetic vortex, is also found to be a ground state of ferromagnetic disk-shaped nanodots with thickness L and radius R , when $L > \xi_{\text{ex}}$, and $R \gg \xi_{\text{ex}}$.^{4–10} This essentially nonlinear state can be interpreted as a part of a two-dimensional (2D) magnetic topological soliton¹¹ adapted to the dot shape. Experimental studies of the vortex state in ferromagnetic nanodots have been performed using magnetic force microscopy,^{4,5} Lorentz microscopy,^{5,6} and magneto-optical techniques.^{7–9} Analytical and numerical micromagnetic modeling of magnetization reversal due to magnetic vortex formation and its displacement have also been carried out.¹⁰

The dynamic properties of such dots have, however, drawn less attention. There are two distinct issues in magnetization dynamics. One concerns the dynamics of magnetization reversal that describes the time evolving magnetization; typically a nonequilibrium state induced by the application of a field pulse. Experimental investigations of the magnetization dynamics under short field pulses include studies of saturated FeNi dots¹² and closure domains in Co dots.¹³ The second issue concerns the dynamics of the spins in the vicinity of an equilibrium state that determines the excitation spectrum. The purpose of the present work is to investigate spin excitations within magnetic vortices. This is quite distinct from the problem of the dynamics of magnetization reversal in which the “magnetization curling” is one of the nucleation modes and which has been addressed earlier.^{2,3}

Spin excitations in the vortex state are expected to be substantially different from those in the uniformly magnetized state. An example is the appearance of a low-frequency mode associated with the displacement and movement of the vortex as a whole. It was found¹⁴ that, when the in-plane field is varied, the vortex core undergoes a spiral motion. The frequency of this motion lies in the sub-GHz range for thin submicron dots. This type of mode is, however, in a cross-over region between field-driven magnetization dynamics and magnon dynamics. In a broad sense this mode is roughly equivalent to a domain-wall resonance in a magnetic film.¹⁵ Excitations of the vortex state have been discussed for infi-

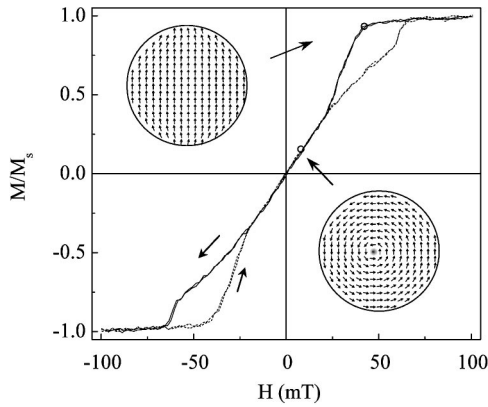


FIG. 1. Measured in-plane hysteresis curve for the array of permalloy disks investigated ($L=60$ nm, $R=400$ nm).

nite films¹⁶ taking into account only the exchange interaction. This is, however, an unsuitable approximation for magnetization dynamics of submicron magnetic particles, where the exchange contribution to the low-lying eigenfrequencies is smaller than the magnetostatic contribution ($R \gg \xi_{\text{ex}}$). The magnetization dynamics in this case is governed by the long-range dipolar forces arising from oscillations of surface and volume magnetic charges. We are not aware of any theoretical or experimental investigation of dipole dominated spin excitations in a magnetic vortex state. By analogy with spin dynamics in thin films, the frequency range of such excitations is expected to be comparable to that probed by ferromagnetic resonance (FMR), and therefore it can be studied using the Brillouin light-scattering technique.

The array of dots with nominal diameter $2R=800$ nm and thickness $L=60$ nm, arranged on a square lattice with a period of $1.6 \mu\text{m}$, was prepared using electron-beam lithography and lift-off techniques. The hysteresis loop for this array, shown in Fig. 1, is typical for dots that undergo magnetization reversal via formation of a vortex state. Details of the sample fabrication, and magneto-optical Kerr effect (MOKE) characterization of its vortex ground state have been given in Refs. 9 and 17.

Brillouin spectra were recorded on a five-pass Fabry-Perot interferometer.¹⁸ The incident and scattered beams were at 45° and 0° from the substrate normal, respectively. Although, due to the very weak signals, the quality of the spectra was not optimal, it was possible to track the peak positions as a function of applied field. In Fig. 2 we show two Brillouin spectra. After saturating at high fields, the field was reduced to 50 mT (upper plot), i.e., in the saturated state above the nucleation field, and at 20 mT (lower plot) with the sample in the vortex state. Two modes are always observed in the vortex state. Three modes are observed in the saturated state at 50 mT but they coalesce and become unresolved at higher fields. The measured frequencies are plotted as a function of field in Fig. 3. Full symbols correspond to the vortex state, and open symbols to the saturated state. We concentrate below on the modes observed in the vortex state. The high-field measurements and quantitative description of the spin excitations for in-plane saturated dots were reported in

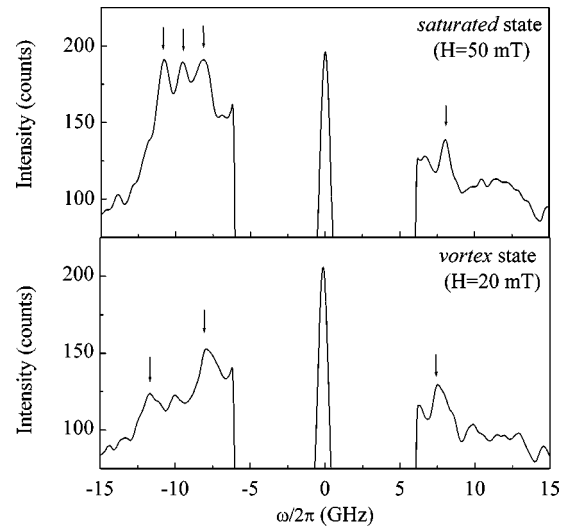


FIG. 2. Brillouin spectra obtained after saturating the sample at high fields and then reducing it to 0.5 kOe (upper plot), i.e., in the saturated state above the nucleation field, and at 0.2 kOe (lower plot) with the sample in the vortex state.

Refs. 19 and 20. For the vortex state considered here the excitations should reflect the circular symmetry of the static distribution of magnetization and dipolar field, as opposed to the uniaxial symmetry of excitations in the saturated state.²¹

In order to interpret the experimental data on spin dynamics in a magnetic vortex trapped in a circular ferromagnetic dot, we have performed micromagnetic calculations based on a Landau-Lifshitz-Gilbert (LLG) equations approach.²² The material parameters are: the saturation magnetization $M_s = 8.0 \times 10^5$ A/m, and the exchange stiffness constant $A = 1.3 \times 10^{-11}$ J/m. The dot diameter and thickness are 800 and 60 nm, respectively. In our 2D calculation, the particle is composed of 6×6 nm interacting cells. The dynamics of each element obeys the LLG equations, which describe the response of a “spin” to an effective magnetic field consisting

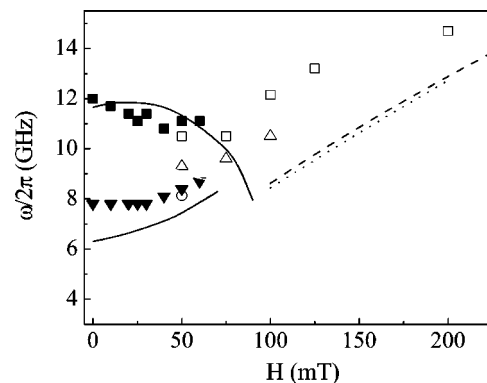


FIG. 3. The symbols are the frequencies obtained from Brillouin spectra like those in Fig. 2. The solid and dashed lines are micromagnetic simulations, the dotted line is the calculation using Kittel's equation for the saturated sample, as explained in the text. The symbols with different shapes correspond to different experimental points obtained from Stokes- and anti-Stokes parts of the BLS spectra.

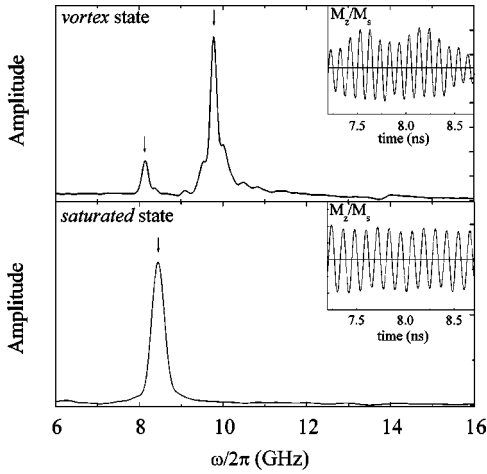


FIG. 4. The peaks in the Fourier transform (FT) correspond to the frequencies of the normal modes of the system. The time-dependent oscillation of magnetization is shown in the inset.

of the exchange coupling from its neighboring cells, magnetostatic fields resulting from the divergence of magnetization \mathbf{M} , and an applied external field \mathbf{H} .

First, we calculate the spin distribution in the presence of an in-plane magnetic field H_x in the range from 0 to 250 mT and a small magnetic field $H_z = 5$ mT applied perpendicular to the dot plane. During this portion of the calculation the damping coefficient α is set to 0.1 in order to quickly relax the magnetization to its equilibrium state. The resulting spin configuration is then used as an initial state for the following calculation of spin dynamics. Retaining the value of H_x , and setting $H_z = 0$ to zero and α to 1×10^{-4} (in order to have underdamped precession), the time dependencies of M_x , M_y , and M_z were recorded. Typical outputs are shown for M_z in the inset to Fig. 4. When the in-plane field H_x exceeds the value of the annihilation field and the vortex is swept out of the dot, and we obtain information on the magnon frequencies in the saturated, single-domain state.

The Fourier transform (FT) of the magnetization oscillations, shown in Fig. 4, yield the corresponding eigenfrequencies of the spin excitations. Note that with conventional micromagnetic codes, such as the one used here,²¹ it is only possible to observe spin excitations for which the spatial average of the time-dependent magnetization is nonzero. The most intense peaks in the FT of M_z and M_y are shown in Fig. 3. Full lines correspond to the vortex state and the dashed lines are for the saturated state. We can also calculate the FMR frequency using the Kittel's equation $\omega_{\text{FMR}}^2 = \gamma^2 H \{ H + 4\pi M_s [1 - 3F(\beta)] \}$, where $F(\beta)$ is average in-plane demagnetizing factor of a saturated circular dot with an aspect ratio $\beta = L/R$. For $\beta = 0.15 \ll 1$, $F(\beta) \approx 2\beta [\ln(8/\beta) - \frac{1}{2}] = 0.083$.¹⁰ Agreement between the micromagnetic and calculated FMR frequency (dotted line) in Fig. 3 is a clear indication that the use of micromagnetics to extract dynamic properties is valid. The experimentally observed frequencies in the saturated state (open symbols) have been identified as standing-wave excitations.¹⁹ This explains why they lie above the FMR frequency. The micromagnetic calculations also reproduce the general trends of the experimental data in

the vortex state. Calculations performed for dots with different thickness and radii show that the frequencies of the two modes in vortex state are strongly dependent on the dot aspect ratio $\beta = L/R$, consistent with expected magnetostatic nature of the observed spin excitations.

To consider the effect of the exchange interaction on the frequencies of these excitation modes we performed additional micromagnetic calculations where we treat the exchange stiffness constant A as a variable. Although the exchange constant has a clear effect on the structure of the vortex core, the frequency of higher excitation mode (12 GHz) appears to be essentially independent of A , whereas the frequency of lower mode increases only slightly with decreasing A . This supports the validity of our assumption about the magnetostatic nature of the observed excitations, especially the quasiuniform mode.

Spin deviations from their equilibrium position result in restoring torques due to exchange, Zeeman, and demagnetizing fields. The magnitude of the torque determines the excitation frequencies. Note that real microfabricated dots (that are not ellipsoids of revolution) have an inhomogeneous demagnetizing field. It may lead to magnetostatic spin excitations that have spatially varying amplitudes near the vortex core, in the central area of the dot, and at the edges. This was confirmed by plotting the time evolution of the profile of the out-of-plane magnetization component (not show here). Indeed, one can clearly see that the spins located far from the edge and from the vortex core behave collectively, and have in-phase precession, reminiscent of a uniform excitation mode. The period of this oscillation corresponds to our higher-frequency (12 GHz) mode. On other hand, the spins located at the dot edges show a different behavior. Their M_z component, as obtained with micromagnetic solver, has a maximum amplitude at the dot edge (where $\rho = R$, R is the dot radius) and decreases toward the dot center. The frequency of this edge-localized mode is lower than that of quasiuniform mode and is at ~ 6.5 GHz (vs 7.8 GHz in the experiment). A theoretical solution to the general problem of magnetic excitations in a vortex state has not yet been reported. However, by making approximations suitable for the low-lying excitations investigated here, the problem can be addressed analytically as described below.

By analogy with excitations in thin films we expect that dynamic exchange contributions to the long-wavelength mode frequencies will be small. Furthermore, due to the small radius of the vortex core ($\xi_{\text{ex}} \ll R$) we can assume that the contributions of the vortex core region to the dynamic magnetization will also be small. Within this approximation, the static magnetization (in cylindrical coordinates) can be written as $\mathbf{m}_0 = (0, m_\varphi^0, 0)$ and the dynamic part $\boldsymbol{\mu}$ of the magnetization (associated with the spin precession about the equilibrium direction) as $\boldsymbol{\mu} = (\mu_\rho, 0, \mu_z)$. Restricting the discussion to the zero applied field case, and considering only modes that have radial symmetry and are uniform along the cylinder, the total "dynamic" energy (W) can be written as

$$W = -\pi L \int d\rho \rho \mathbf{H}_m(\rho) \cdot \mathbf{M}(\rho), \quad \mathbf{M} = \mathbf{m} M_s. \quad (1)$$

The magnetostatic field, $\mathbf{H}_m=(H_\rho, 0, H_z)$, can be expressed via a tensorial magnetostatic Green's function $G_{\alpha\beta}(r, r')$ with $(\alpha, \beta=\rho, \varphi, z)$.²³ Due to the radial symmetry of $\mathbf{m}(\rho)$, only the $\rho\rho$ and zz components of the $G_{\alpha\beta}(r, r')$ are nonzero. The equation of motion for the magnetization components $-(M_s/\gamma)\partial\mathbf{m}/\partial t=\mathbf{m}\times(\partial w/\partial\mathbf{m})$, where w is the energy density corresponding to the magnetostatic energy in Eq. (1), can be linearized by substitution with $\mathbf{m}(\rho, t)=\mathbf{m}_0(\rho)+\boldsymbol{\mu}(\rho, t)$.

For small amplitudes of the $\boldsymbol{\mu}$ components, we get a system of two coupled linear integral equations of Fredholm type²⁴ with kernels expressed via the $g_{\rho\rho}$ and g_{zz} components of the averaged $G_{\alpha\beta}(r, r')$ tensor. The solution of this problem for a thin disk yields a discrete set of magnetostatic eigenfunctions $\mu_n(\rho)$ and corresponding eigenfrequencies ω_n as follows:

$$\left(\frac{\omega_n}{\omega_M}\right)^2 = -\frac{1}{4\pi} \int_0^R \rho \int_0^R \rho' g_{\rho\rho}(\rho, \rho') \mu_n(\rho) \mu_n(\rho') d\rho d\rho' \quad (2)$$

with $g_{\rho\rho}(\rho, \rho') = -4\pi \int_0^\infty k f(kL) J_1(k\rho) J_1(k\rho') dk$, $\omega_M = \gamma 4\pi M_s$, and $f(x) = 1 - (1 - e^{-x})/x$.

From Eq. (2) we obtain $\omega_n^2 = \omega_M^2 I(L/R)$, where the function $I(x)$ depends only on the dot aspect ratio and on the magnetization distribution of the normalized to unit n eigenmode $\mu_n(\rho)$. The eigenfunctions $\mu_n(\rho)$ are orthogonal with real eigenvalues because the kernel $g_{\rho\rho}(\rho, \rho') = g_{\rho\rho}(\rho', \rho)$ is symmetric and real.²⁴ The function $I(x)$ to a good approximation is linear in L/R and therefore we get the simple relation $\omega_n \propto (L/R)^{1/2}$. These frequencies are well above the translational mode eigenfrequency $\omega = (5/9\pi)\omega_M(L/R)$ calculated in Ref. 14. Accounting for the azimuthal dependence

of the dynamic magnetization will result in additional contributions from the magnetostatic and exchange interactions, which will lead to higher eigenfrequencies than considered herein. The function $g_{\rho\rho}(\rho, \rho')$ has a sharp maximum near the point $\rho = \rho'$. The eigenfunctions in Eq. (2) are approximately proportional to the ρ component of the dynamic dipolar field. If we assume that $\mu_n(\rho)$ is localized at the dot edge $\rho = R$, then we can get, in a self-consistent way $\mu_n(\rho) \sim g_{\rho\rho}(\rho, R)$ and find the corresponding eigenfrequency. For permalloy dots with $M_s = 800$ G, $L = 60$ nm, $R = 400$ nm, $\gamma/2\pi = 2.95$ GHz/kOe, and $\omega_M/2\pi = 29.7$ GHz the expression (2) yields an approximate eigenfrequency of 8.6 GHz for this mode. We get an approximate eigenfrequency of 14.4 GHz for an almost uniform amplitude profile $\mu(\rho) \cong \sqrt{2}/R$. More exact mode profiles should be found from the solution of the integral equation with the kernel $g_{\rho\rho}(\rho, \rho')$.

Both the calculated modes are magnetostatic in nature and are concentrated in the area outside of the vortex core. Full details of the analytical model procedure will be reported elsewhere.

In summary, we experimentally show that in the vortex state, in addition to translational mode, there are other excitation modes, whose frequencies are determined principally by dynamic demagnetizing fields. By comparing our experimental results and micromagnetic calculations we are able to conclude that these modes correspond to the excitation mainly at the dot edge and another that is fairly uniform over the disk diameter.

Work at Argonne was supported by U.S. Department of Energy, BES Materials Sciences, under Contract No. W-31-109-ENG-38.

¹A. Hubert and R. Schäffer, *Magnetic Domains: The Analysis of Microstructures* (Springer-Verlag, Berlin-Heidelberg, 1998).

²A. Aharoni, *Phys. Status Solidi* **16**, 3 (1966).

³R. Skomski *et al.*, *Phys. Rev. B* **60**, 7359 (1999).

⁴T. Shinjo *et al.*, *Science* **289**, 5481 (2000).

⁵J. Raabe *et al.*, *J. Appl. Phys.* **88**, 4437 (2000).

⁶M. Schneider *et al.*, *Appl. Phys. Lett.* **77**, 2909 (2000).

⁷R. P. Cowburn *et al.*, *Phys. Rev. Lett.* **83**, 1042 (1999).

⁸C. A. Ross *et al.*, *Phys. Rev. B* **65**, 144417 (2002).

⁹V. Novosad *et al.*, *Phys. Rev. B* **65**, 060402 (2002).

¹⁰See the following and references therein, K. Yu. Guslienko *et al.*, *Phys. Rev. B* **65**, 024414 (2002).

¹¹A. M. Kosevich *et al.*, *Phys. Rep.* **194**, 117 (1990).

¹²W. K. Hiebert *et al.*, *Phys. Rev. Lett.* **79**, 1134 (1997).

¹³Y. Acremann *et al.*, *Science* **290**, 492 (2000).

¹⁴K. Yu. Guslienko *et al.*, *J. Appl. Phys.* **91**, 8037 (2002).

¹⁵B. E. Argyle *et al.*, *Phys. Rev. Lett.* **53**, 190 (1984).

¹⁶See the following and references therein, B. A. Ivanov *et al.*, *Phys. Rev. B* **58**, 8464 (1998).

¹⁷M. Grimsditch *et al.*, *Phys. Rev. B* **65**, 172419 (2002).

¹⁸The Brillouin spectrometer was a tandem system used in five-pass mode to improve the transmission and thereby make the very weak signals observable.

¹⁹S. O. Demokritov and B. Hillebrands, in *Spin Dynamics in Confined Magnetic Structures I*, edited by B. Hillebrands and K. Ounadjela (Springer, Berlin, 2002).

²⁰M. Grimsditch *et al.*, *Phys. Rev. B* **58**, 11539 (1998).

²¹W. K. Hiebert *et al.*, *Phys. Rev. B* **65**, 140404 (2002).

²²M. J. Donahue and D. G. Porter, OOMMF User's Guide, Interagency Report NIST IR 6376. National Institute of Standards and Technology, Gaithersburg, MD (Sept. 1999).

²³K. Yu. Guslienko and A. N. Slavin, *J. Appl. Phys.* **87**, 6337 (2000).

²⁴H. Hochstadt, *Integral Equations* (Wiley, New York, 1989).